

Intravital Imaging and Photoswitching in Tumor Invasion and Intravasation Microenvironments

Bojana Gligorijevic^{1,2*}, David Entenberg^{1,2}, Dmitriy Kedrin¹, Jeffrey Segall^{1,2}, Jacco van Rheenen^{1,3}, and John Condeelis^{1,2}

¹Department of Anatomy and Structural Biology, Albert Einstein College of Medicine of Yeshiva University, 1300 Morris Park Avenue, Bronx, New York, NY 10461, USA

²Gruss Lipper Biophotonics Center, Albert Einstein College of Medicine of Yeshiva University, 1300 Morris Park Avenue, Bronx, New York, NY 10461, USA

³Hubrecht Institute-KNAW and University Medical Center Utrecht, Uppsalalaan 8, 3584CT Utrecht, Netherlands

* bojana.gligorijevic@einstein.yu.edu

Introduction

Our group studies the spread of cells in primary breast tumors to distant sites, a process that is called metastasis. In order to metastasize, cells migrate and invade the surrounding areas (invasion) and enter the blood (intravasation). Previously, we developed techniques to visualize these cell movements in mammary tumors of living mice at single-cell resolution [1–3]. These techniques involved intravital imaging of carcinomas in which tumor cells express genetically encoded fluorophores such as CFP or GFP [4] using multiphoton microscopy. In contrast to widefield or confocal microscopy, high-contrast images of features several cell diameters deep inside the tissue can be acquired with multiphoton microscopy without tumor dissection and removal from the animal. Using this technology, we were able to simultaneously monitor tumor cells and several components of the tumor microenvironment, such as collagen fibers, blood vessels, and several subpopulations of macrophages. The results of our studies demonstrated that the primary tumor is not just a collection of cells where every cell is equally able to metastasize, but that only a small population of tumor cells is capable of moving rapidly. These fast, invasive cells were seen to invade surrounding tissue, crawl along collagen fibers [5], interact with perivascular macrophages forming a paracrine loop [2], as well as enter into blood vessels (intravasation) under the guidance of macrophages [1]. Based on these data, we were able to identify two separate microenvironments in the mammary carcinoma: the invasion and intravasation microenvironments.

Methods and Materials

In order to test the influence of different tumor microenvironments on the initial steps of metastasis, it is important to visualize the whole sequence: the detachment of the tumor cell from the tissue to migration through the tissue and crossing the blood vessel wall. Unfortunately, these processes take place over days and our imaging sessions could extend maximally up to several hours (up to 24 hours in [6]) due to dehydration of the tissue after skin removal. Moreover, the imaging preparation was a terminal procedure, and therefore most conclusions of intravital imaging studies were made via combining information extracted from different animals [7–9].

To tackle the mechanism of intravasation in more detail, our next step was to monitor the long-term fate of tumor cells and correlate it with their microenvironment. We searched for a way to monitor the behavior of tumor cells in different

regions in the tumor (with different microenvironments) on the time scale of days. Ideally, this would be done over multiple short imaging sessions in which the animal was exposed to anesthetics for only a few minutes because exposure to anesthesia may induce side effects. Importantly, the microenvironment of breast tissue is different from other parts of the body, which makes it critical to study orthotopic tumors (in the mammary fat pad) in contrast to commonly used subcutaneous tumors. In order to do this, we have recently developed a Mammary Imaging Window (MIW) [10, 11]. The window is commonly inserted on top of the palpable tumor (Figure 1A–D). The MIW consists of a plastic mount with

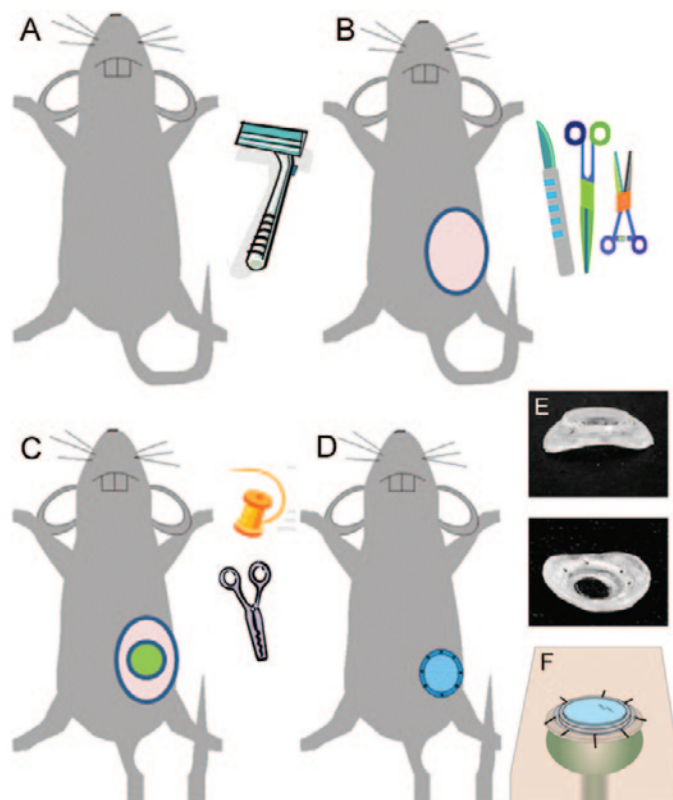


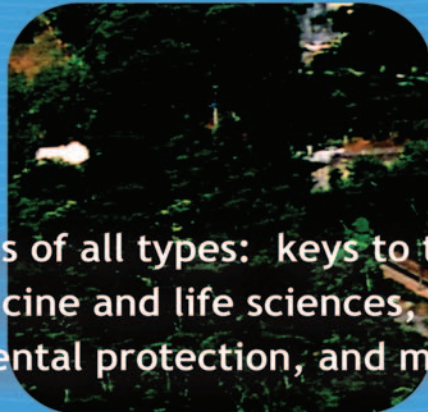
Figure 1: Surgical implantation of the mammary imaging window: (A–D) In order to implant the MIW on top of the mammary tumor, hair is removed from the implantation site, an incision is made in the skin, the underlying connective tissue is detached using sterile instruments, and the window is placed and sutured under the skin. (E) The side and bottom views of the MIW. (F) View of the MIW as it would appear sutured into the skin (beige) on top of a growing tumor.



The IFSM International Microscopy Congress

IMC17

Revealing the Nanoworld in Life and Materials Sciences



Microscopy methods of all types: keys to the frontiers of nanotechnology, medicine and life sciences, microelectronics, energy, environmental protection, and much more . . .

2010

Rio de Janeiro
September 19-24

Organized by the Brazilian Society
for Microscopy and Microanalysis (SBMM)

Under the auspices of the International
Federation of Societies for Microscopy (IFSM)

www.imc17.com

IFSM



evenly distributed holes to facilitate suturing into the skin and a glass coverslip attached on the top, which assures the optimal working distance for high-resolution imaging (Figure 1E–F). In order to insert the window, animals were anesthetized, the hair was shaved off, and an incision was made in the skin. A sterile MIW was inserted and sutured into the skin. After a few days of recovery, the immune response to the surgery diminishes and the animal can be used over many days, where the time limitation comes from the tumor growth [10]. The insertion of the MIW does not influence the tumor because tumors with the MIW implanted do not show significant differences in rate of tumor growth, macrophage density, angiogenesis, or necrosis compared to tumors without the implant. Importantly, the MIW implant allows us to study orthotopic tumor xenografts and transgenic animals growing breast carcinomas.

An animal with a properly implanted MIW and a growing tumor, however, is not enough for a successful imaging session. In order to record intravital tumor cell migration, we need the animal to be properly positioned on the microscope stage, where the coverslip is flat and stable above the objective; also, the animal should be immobilized and breathing stably to avoid artifacts in 3D reconstructions of image *z*-series. To immobilize and position the animal, we placed the mouse inside the custom-designed, stereotactic imaging box (Figure 2). A flow of anesthesia enters the box (Figure 2A) [10] through the inlet positioned in the front of the box and exits on the side (outlet) towards the vacuum, passing through a carbon filter, which removes isoflurane (gas anesthetics) from the isoflurane/oxygen mix. The box lid and sliding doors are lined with sponge cushions to assure that no outside air gets into the box and to protect the animal skin around the MIW. Flexible design of the imaging box bottom frame assures that it can always be mounted in the same position on any type of microscope stage (Figure 2B). Thus, we can always visualize

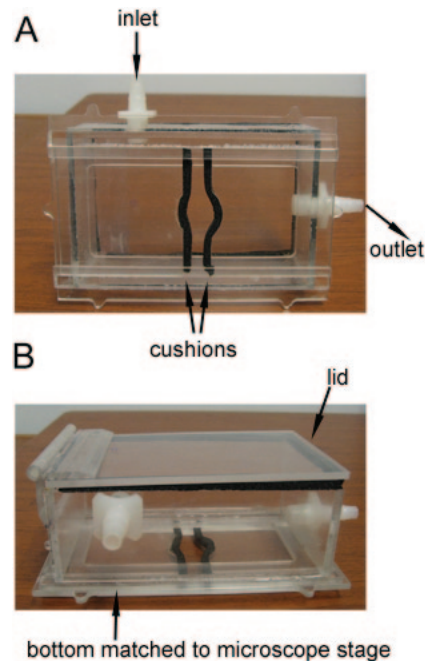


Figure 2: Design of the stereotactic imaging box. (A) Bottom and (B) side view of the box fabricated out of 1/8-inch Plexiglas.

the same general area of the tumor throughout imaging sessions.

However, as the tissue topology of the tumor changes due to angiogenesis and cell proliferation and migration, the use of the stereotactic box does not assure that we will be looking at the same group of cells each time we put the animal on the stage (Figure 3A–B). In order to recognize specific groups of cells, or even specific tumor cells each time, we need a more precise, internal landmark. For this purpose, we

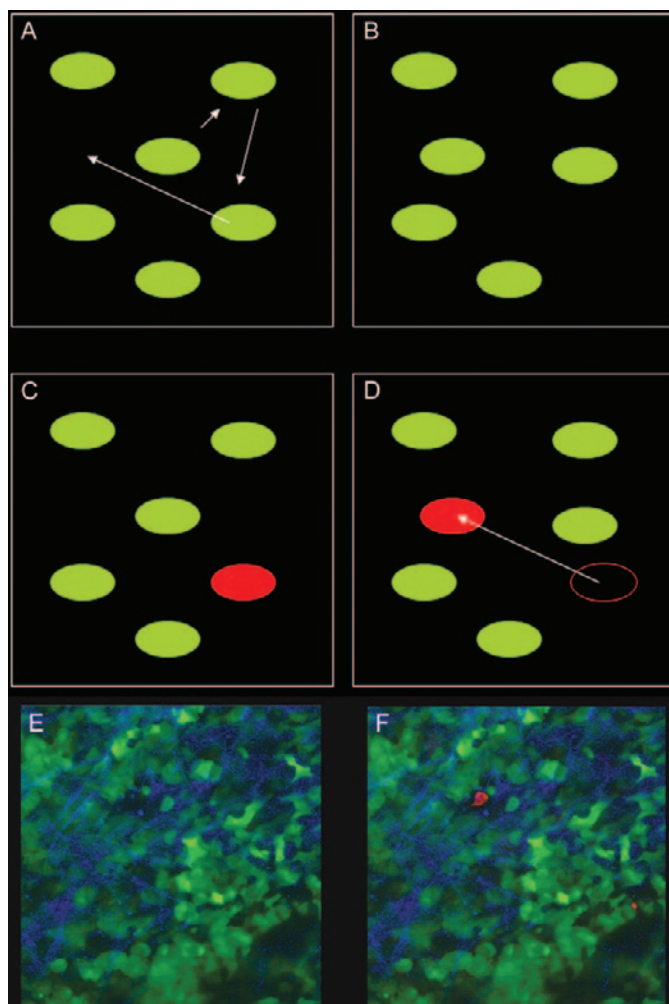


Figure 3: The principle of photoswitching. (A, B) Constant movement and reorganization of tumor cells makes it impossible to determine their itinerary over two or more imaging sessions. (C, D) However, by changing the color of chosen cell(s) from green to red, we can determine start and end positions. (E–F) Example of a photoswitched tumor cell inside a living animal: extracellular matrix is shown in blue, non-switched cells in green, and “photoswitched” tumor cell in red.

genetically incorporated a photoswitchable protein Dendra2 as a cytoplasmic cell marker into some tumor cells. The presence of Dendra2 protein makes cells fluoresce in green, similarly to commonly used GFP-labeled cells. However, if we briefly illuminate one or more cells with a 405-nm laser (alternatively, 820 nm can be used for photoswitching in multiphoton), fluorescence of those cells switches from green to red, without changing their phenotype otherwise (Figure 3C–D) [12]. With the use of this approach, at each of the time points in the experiment, we collect images of total tumor cell population in the green channel, as well as images of the tumor cell(s) of interest in the red channel. The choice of the size of photoswitched area depends on the experimental design and can be as small as one single cell (Figure 3E–F) or as large as an entire field of view (1,000–1,500 cells with 20× objective).

Results

To test the influence of the intravasation microenvironment on the surrounding cells, we can photoswitch tumor cells in regions of interest in the vicinity

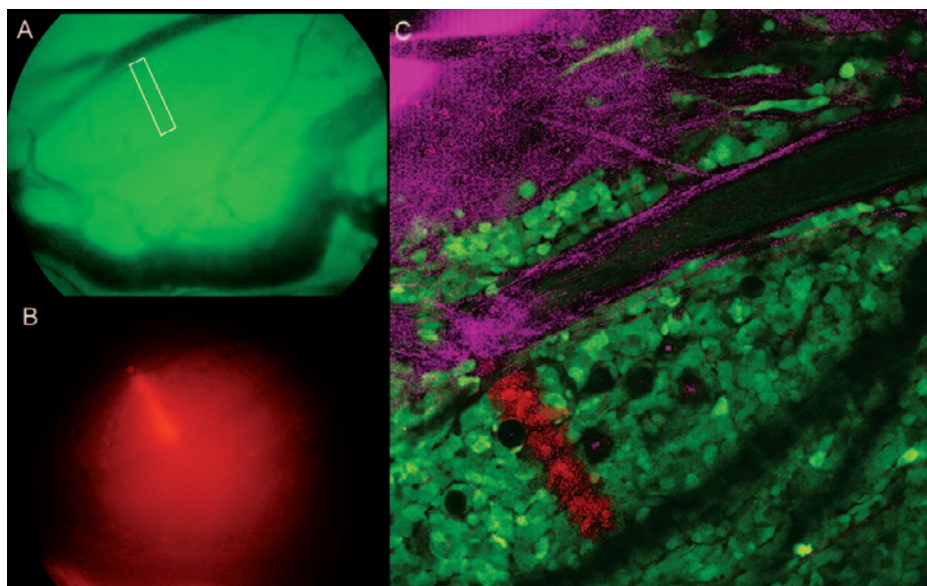


Figure 4: Example of intravital imaging and photomanipulation in tumor intravasation microenvironment. (A) Region of interest (ROI) to be photoswitched is chosen using 10 \times ocular view through the MIW in the green channel; in the image, the ROI is perpendicular to a flowing blood vessel (white outline). (B) Same field viewed in red channel after the photoswitching. (C) High-resolution image of the tumor microenvironment after photoswitching: Dendra2-MDA-MB-231 cells (green), extracellular matrix (purple), blood vessels (black), and photoswitched region (red). Scale 25 μ m.

of blood vessels (Figure 4, 5). This way, we are able to monitor fates of hundreds of cells simultaneously. As cells in the tumor migrate and invade, the distribution of these (red) cells relative to blood vessels and other cells changes; this can be quantified as change in cell position or in number of red cells present in

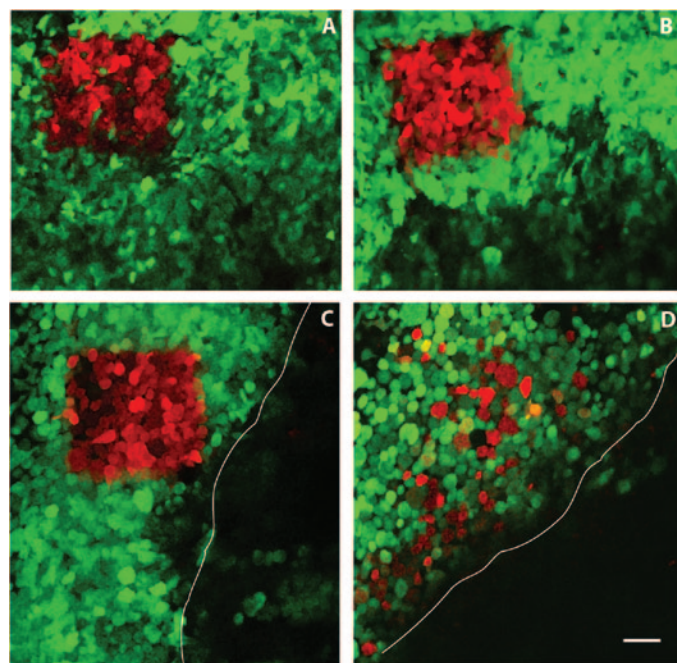


Figure 5: Tumor intravasation microenvironment dictates the behavior of tumor cells. (A, C) show two regions of interest (ROI) photoswitched at 0h in the same animal. (B) At 24h, region far from a major blood vessel shows almost no change in cell position and number. (D) At 24h, region next to a major blood vessel shows dispersion, alignment around the vessel and a decrease in cell number. Color code: Dendra2-MDA-MB-231 cells (green), blood vessel (unlabeled, white outline) and photoswitched cells (red). Scale 30 μ m.

the region [10, 11] over multiple days [13]. Figure 5 demonstrates that tumor cell behavior is in fact guided by the surrounding microenvironment and that the vascular microenvironment promotes intravasation of tumor cells. Tumor cells that are only several cell diameters away from each other behave differently depending on their distance to a blood vessel. We are currently working on correlating the behavior of individual tumor cells or tumor cell populations to different types of microenvironments within the tumor.

However, many new questions were opened by this result, such as: what are the borders of the invasion and intravasation microenvironments? Is the existence of the microenvironment time-dependent? How many components of the tumor tissue are involved in the microenvironment formation? Can we develop microenvironment-specific drugs? [14]

References

- [1] J Wyckoff et al., *Cancer Res* 67 (2007) 2649.
- [2] J Wyckoff et al., *Cancer Res* 64 (2004) 7022.
- [3] J Wyckoff, B Gligorijevic, J Segall, and J Condeelis, *Live Cell Imaging: a Laboratory Manual*, Cold Spring Harbor, NY, 2009.
- [4] E Sahai, J Wyckoff, U Phillipar, J Segall, F Gertler, and J Condeelis, *BMC Biotechnol* 5 (2005) 14.
- [5] M Sidani, J Wyckoff, C Xue, JE Segall, and J Condeelis, *J Mammary Gland Biol Neoplasia* (2006) 151.
- [6] M Egeblad, AJ Ewald, et al. *Dis Model Mech* 1 (2008) 155.
- [7] J Condeelis, JE Segall, *Nat Rev Cancer* 3 (2003) 921.
- [8] RM Hoffman, *Nat Rev Cancer* 5 (2005) 796.
- [9] RK Jain, LL Munn, D Fukumura, *Nat Rev Cancer* (2002) 266.
- [10] D Kedrin, B Gligorijevic, et al., *Nat Methods* 5 (2008) 1019.
- [11] B Gligorijevic, D Kedrin, et al., *Jove* 28 (2009) doi: 10.3791/1278.
- [12] NG Gurskaya et al., *Nat Biotechnol* 24 (2006) 461.
- [13] B Gligorijevic, J Condeelis, *Cell Adh Migr* (2009) 313.
- [14] This research is supported by the DOD BC075554 (BG), NIH U54CA126511 (JC, BG), and NIH CA100324 (DE, JC).

MT

